

Line-Based Modulation Transfer Function Measurement of Pixelated Displays

KENICHIRO MASAOKA 

NHK Science and Technology Research Laboratories, Tokyo 157-8510, Japan

e-mail: masaoka.k-gm@nhk.or.jp

ABSTRACT This paper proposes a line-based method for measuring the modulation transfer function (MTF) of a display. In this method, the spatial distribution of a single line that is displayed in a small region of the screen is analyzed. This is performed by capturing the displayed line by a light measuring device (LMD). The square sampling grid of the LMD is set slightly slanted relative to the displayed line so that the line is recorded with various offsets with respect to the sampling positions. By analyzing a supersampled 1D line spread function generated from a small region of interest (ROI) in the image of the captured line, the display MTF is estimated. The convolution theorem is used to compensate the display MTF for the underestimation related to the spatial performance or MTF of the LMD. Thereby, accurate display MTF results are obtained for a wide range of pixel ratio, i.e., the number of pixels of the measurement device per display pixel interval. The proposed method was validated using computer-generated images of a model display with an RGB stripe subpixel arrangement and a model LMD. The utilization of a low pixel ratio enables the measurement to be performed using a small lens and long working distance. In addition, the small size of the employed ROI significantly reduces the computational cost and allows the use of a low-resolution camera.


INDEX TERMS Digital display, light measuring device, modulation transfer function.

I. INTRODUCTION

Ultrahigh definition (UHD) technology produces visually realistic digital images [1]. UHD devices are usually categorized by the horizontal pixel counts of the standard image formats of their input/output signals, such as 4K and 8K. However, the spatial imaging performance of a display is typically not solely determined by the pixel count. Although traditional flat-panel displays use separate red, green, and blue (RGB) micro-color-filter elements within each pixel, such as in RGB stripe patterns, some recent display technologies do not use these three colors for each incoming image pixel, obscuring the pixel count [2]. Although some projectors use a wobulation technique that increases their apparent resolutions, their spatial resolution characteristics are usually inferior to those of full-resolution projectors. Furthermore, the optical elements used in a display structure affect the spatial imaging performance. For example, a diffusing film can be overlaid on the front surface of a panel to improve the viewing angle and reduce the specular reflection of ambient light. However, such front surface diffusers generate

interpixel crosstalk and sparkle, which degrade the spatial resolution characteristics of the display.

The International Committee for Display Metrology (ICDM) recommends the use of the Michelson contrast of the luminance of a displayed alternating black-and-white line-pair pattern, so-called contrast modulation [3], for determining the spatial resolutions of displays. The Consumer Technology Association (CTA) in the USA also adopts contrast modulation as the industry benchmark for 8K UHD displays [4]. However, the measurement precision of contrast modulation is affected by the sampling offset between the display pixels and the detector array of the light measuring device (LMD). Furthermore, contrast modulation is underestimated when the spatial imaging performance of the LMD is inadequate [5]. Preventing the underestimation usually requires capturing the line-pair pattern at a relatively high magnification. The ICDM recommends a high pixel ratio (number of LMD pixels per display pixel interval) of over 30 for accurate contrast modulation [6]. However, determining the minimum required pixel ratio is not straightforward because it depends on the architecture of the display device, including the display pixel aperture and front surface diffuser, in addition to the spatial performance of the LMD [5].

The associate editor coordinating the review of this manuscript and approving it for publication was Chao Tan .

The modulation transfer function (MTF) is used to characterize the spatial imaging performance of an imaging system. Based on the convolution theorem, the MTF of the entire system is estimated by multiplying the MTFs of its constituent subsystems.

To measure the modulation transfer value of a display directly for a particular spatial frequency, the ratio of the modulation of the fundamental frequency component in the rendered sinewave to that of the input sinewave is estimated from an image captured by an LMD (e.g., [7]). The MTF of the intermediate LMD can be compensated for based on the convolution theorem. However, the phase of the sinewave must be carefully considered in the case of pixelated displays. Furthermore, displaying a low spatial frequency wave requires a large region on the screen.

Several other display MTF measurement methods involve the analysis of the responses of a line, an edge, periodic bar-patterns, and white noise. Chawla *et al.* [8] compared these methods and found that they yielded practically the same results. However, Chawla *et al.* set a CCD camera to capture the display screen at a very high pixel ratio of 18. Many other researchers also set a camera very close to a display screen and analyzed the responses of a line (e.g., [9], [10]), square waves (e.g., [11]), and a single pixel (e.g., [12]) to minimize the effects of the camera MTF and/or the sampling offset between the display and camera pixels on the estimates of display MTF.

The ICDM recommends a display MTF measurement method that involves analysis of the response of a single bitonal edge pattern in a small region. In this edge-based method, a vertical or horizontal edge is displayed on the screen and then captured by an LMD. The square sampling grid of the LMD is slightly slanted relative to the displayed edge to record the edge in various offsets or phases with respect to the sampling positions of the LMD. A 1D super-sampled edge profile is generated from the captured edge image. The edge profile with fluctuations due to the subpixel arrangement of the display is smoothed by a wavelet-based denoising technique and differentiated to yield a line profile. The MTF is then estimated from the line profile. However, the denoising algorithm is not sufficiently documented, and the effect on the MTF results should be clarified. Furthermore, it seems unnecessary to start by analyzing the edge response because the line profile can be directly obtained from a line displayed on the screen.

To address the challenges of the existing methods, this paper provides the MTF concept for sampled imaging systems and proposes a new line-based MTF measurement method that utilizes the convolution theorem. This method involves analysis of the spatial distribution of a single line displayed in a small region of the screen and eliminates the need for conversion from an edge profile to a line profile and the accompanying smoothing and denoising processes. The effects of the camera MTF and the sampling offset between the display and camera pixels on the display MTF estimates can be minimized even for very low pixel ratios.

II. MTF CONCEPT

A. MTF FOR LINEAR AND SHIFT-INVARIANT SYSTEMS

The MTF is defined as the magnitude of the response of a system to sinusoids of different spatial frequencies. In the analysis of a linear and shift-invariant (LSI) imaging system consisting of several subsystems, the overall MTF can be calculated by multiplying the MTFs of the subsystems in the frequency domain, based on the convolution theorem. This process eliminates the need for repetitive convolution of the impulse responses in the spatial domain. The MTF is then used as an effective indicator for characterizing the spatial imaging performance.

B. MTF FOR SAMPLED IMAGING SYSTEMS

To preserve the convenience of the transfer function approach for shift-variant sampled imaging systems, the MTF concept for LSI systems has been extended [13].

For digital image capturing devices, the object to be imaged is assumed to be composed of spatial frequency components with random phases that are uniformly distributed relative to the sampling positions. The MTF is subsequently obtained as the average MTF over a statistical ensemble of phases [13]. Based on this idea, the ISO 12233 edge-based method [14] is widely used. The method involves analysis of the edge gradients of an image of a nearly vertical or nearly horizontal knife-edge target slanted with respect to the square sampling grid. The modified edge-based method accommodates any edge orientation (with the exception of critical edge angles, namely, those near 0° , 45° , and 90°) for MTF estimation with higher accuracy and precision [15].

For pixelated display devices, Infante [16] considered the active pixel area as the point spread function and derived the MTF based on the fill factor. In this study, the display MTF is based on this concept, and displays are assumed to be shift-invariant to the “discrete” input image data defined on the sampling grid of the image format. This means that the displayed image is the same all over the effective area of the screen.

C. SPATIAL FREQUENCY AND METROLOGICAL PIXEL

The MTF for a sampled imaging system is a function of the spatial frequency defined in the image format of the input/output signal. An effective metrological method should be independent of the device architecture and be technologically neutral. Therefore, the pixel can be logically defined by the standard image format of the input/output signal and not by the physical pixel of the device. As an example, the ITU Radiocommunication Sector (ITU-R) defined the pixel count and sampling lattice for 4K and 8K UHD formats in Recommendation BT.2020 [17]. The sampling frequency of 1 cycle/pixel is defined by the sampling lattice of the image format. The Nyquist frequency is half of the sampling frequency. For display MTF estimation, the spatial frequency range is limited to 0–0.5 cycles/pixel.

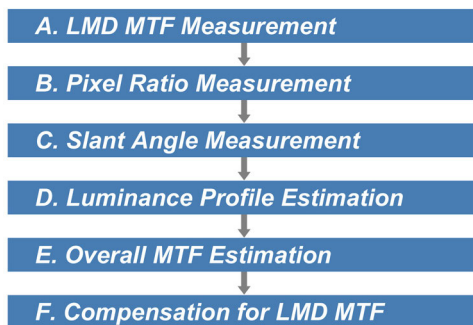


FIGURE 1. Flowchart of line-based display MTF measurement method.

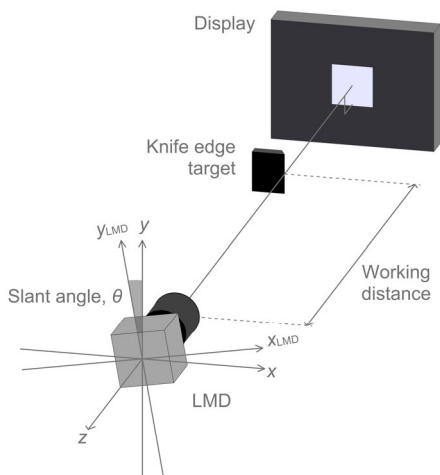


FIGURE 2. Schematic of the edge-based MTF measurement setup.

III. LINE-BASED DISPLAY MTF MEASUREMENT METHOD

The proposed line-based display MTF measurement method involves an analysis of the spatial distribution of a single line displayed in a small region of the screen, which is captured by an LMD.

Fig. 1 shows a flowchart of the method, which consists of six steps. The MTF of the LMD is measured in the first step and compensated for in the estimation of the display MTF in the final step. For this purpose, two spatial frequencies are considered. One is the spatial frequency ξ_{LMD} in cycles/pixel_{LMD}, where pixel_{LMD} is the pixel interval defined in the image format of the output signal of the LMD, and the other one is the spatial frequency ξ_{DISP} in cycles/pixel_{DISP}, where pixel_{DISP} is the pixel interval defined in the image format of the input signal of the display. Herein, the pixel ratio is defined as the ratio of pixel_{DISP} to pixel_{LMD}. The pixel ratio is used for the conversion of ξ_{LMD} and ξ_{DISP} in the final step. Following are descriptions of the steps of the procedure.

A. LMD MTF MEASUREMENT

The MTF of an LMD, which is used to capture the display screen, is measured using the modified edge-based method [18]. The following measurement is performed in a dark room. As shown in Fig. 2, a knife-edge target, that is, a sharp and straight black blade, is positioned in front of

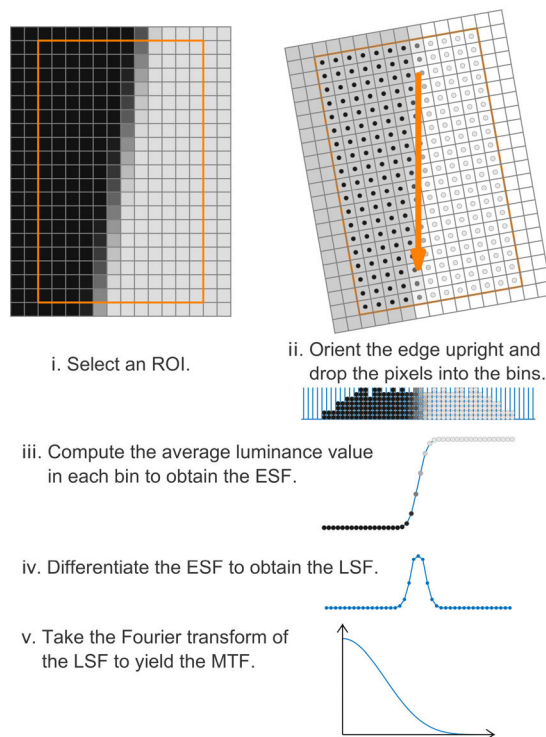


FIGURE 3. Schematic flow diagram of the edge-based MTF measurement method for LMDs. A small ROI and wide bins are used here as simple examples.

the display. The target is backlit by the display being tested. A patch of the same color as the line to be measured is used as a uniform light to properly measure the color-dependent MTF of the LMD. The display is positioned at a distance outside the depth of field so that the patch is uniformly captured without any artifacts caused by the display subpixel array and the sampling array of the LMD. The optical axis of the LMD (z-axis) is set perpendicular to the surfaces of the display screen and edge target, while the LMD is rotated around the optical axis so that the edge is slanted relative to the sampling array of the LMD. The edge orientation should be identical to that of the line to be measured.

Fig. 3 shows a schematic of the algorithm outlined as follows. (i) A region of interest (ROI) is selected on the captured image of the knife edge. In practice, the ROI is selected to enclose the edge on the optical axis. The ROI should therefore be sufficiently small and selected in the central area of the image. (ii) The edge angle in the ROI is estimated by fitting a parameterized 2D cumulative distribution function to the ROI pixel values with significantly high accuracy, precision, and robustness against the camera noise [18]. The ROI is rotated by the estimated edge angle so that the edge is oriented vertically. The ROI pixels are then dropped onto the horizontal axis, which is divided into (pixel_{LMD}/n_{bin})-wide bins to reduce the influence of signal aliasing on the estimated MTF, where n_{bin} is the oversampling ratio, that is, the number of bins per pixel_{LMD}. (iii) The values of the pixels collected from each bin are averaged to generate a supersampled 1D edge spread function (ESF). (iv) A finite difference filter

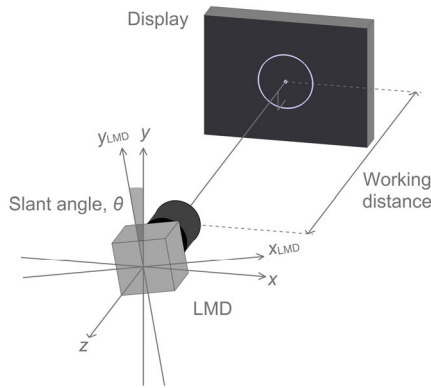


FIGURE 4. Schematic of the pixel ratio measurement setup.

[1/2, 0, -1/2] is then used to approximate the derivative of the ESF to obtain a line spread function (LSF). (v) After applying a Tukey (tapered cosine) window to the LSF for apodization, a discrete Fourier transform is performed to yield the optical transfer function (OTF). The modulus of the OTF is then normalized to unity at zero frequency. The underestimations of the modulus due to the bin-width averaging and the finite difference filter are compensated for by multiplying the normalized modulus times $|\text{sinc}(\xi_{\text{LMD}}/n_{\text{bin}})|^{-1}$ and $|\text{sinc}(2\xi_{\text{LMD}}/n_{\text{bin}})|^{-1}$, respectively [18], [19]. The MTF of the LMD (MTF_{LMD}) is subsequently estimated to be a function of the spatial frequency in the direction perpendicular to the edge in the captured image.

B. PIXEL RATIO MEASUREMENT

The pixel ratio measurement setup is illustrated in Fig. 4. The display to be tested is positioned horizontally at the same working distance as that in the MTF measurement of the LMD. The optical axis of the LMD should be perpendicular to the display screen, and the slant angle and focus position of the LMD should be maintained. An anti-aliased circle of known radius in $\text{pixel}_{\text{DISP}}$ with a dot at its center is then displayed on the screen, and the LMD is used to capture the screen. The captured circle and dot contain unnecessary luminance peaks caused by the arrangement of the micro-color-filter array and black mask of the pixel. To eliminate them, a low-pass filter is applied to the image. Four distances from the center dot to the circle circumference in the vertical (y_{LMD} -axis) and horizontal (x_{LMD} -axis) directions in the smoothed image are estimated. The average distance in $\text{pixel}_{\text{LMD}}$ is subsequently divided by the known radius in $\text{pixel}_{\text{DISP}}$ to obtain the pixel ratio. For example, if a circle of radius 20 in $\text{pixel}_{\text{DISP}}$ is captured as one of radius 100 in $\text{pixel}_{\text{LMD}}$, the pixel ratio would be 5 ($= 100/20$).

C. SLANT ANGLE MEASUREMENT

This process involves estimation of the slant angle of the LMD. Fig. 5 illustrates the setup for capturing the display screen by the LMD. While the display and LMD remain at their positions, a vertical one- $\text{pixel}_{\text{DISP}}$ -wide line is displayed on the screen.

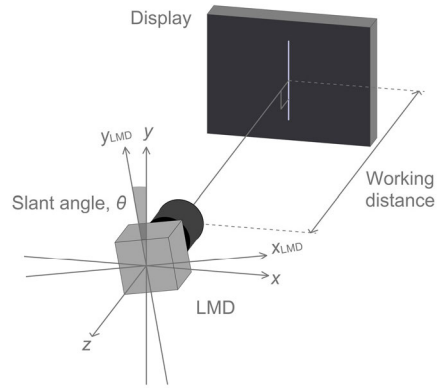


FIGURE 5. Schematic of the slant angle measurement setup.

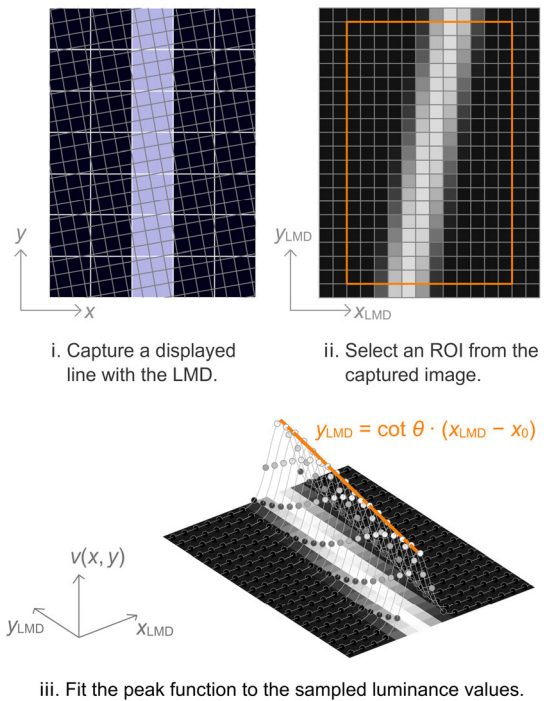


FIGURE 6. Schematic flow diagram of the slant angle measurement process. A small ROI is used here as a simple example.

Fig. 6 illustrates the procedure for estimating the slant angle. (i) The line is captured by the LMD. The slant angle of the line in the captured image is supposed to be identical to that of the edge during the measurement of the MTF of the LMD. The line should be recorded with various phases with respect to the sampling positions of the LMD. (ii) An ROI enclosing the line is selected from the image. Obviously, it is preferable to use the same ROI as in the edge-based LMD MTF measurement to compensate the display MTF estimation correctly for the underestimation due to the MTF of the LMD. (iii) The slant angle θ is estimated from the near-vertical line image by optimizing the following parameterized 2D peak function:

$$v(x_{\text{LMD}}, y_{\text{LMD}}) = \exp[-(x_{\text{LMD}} - x_0 - \tan \theta \cdot y_{\text{LMD}})^2 / 2\sigma^2], \tag{1}$$

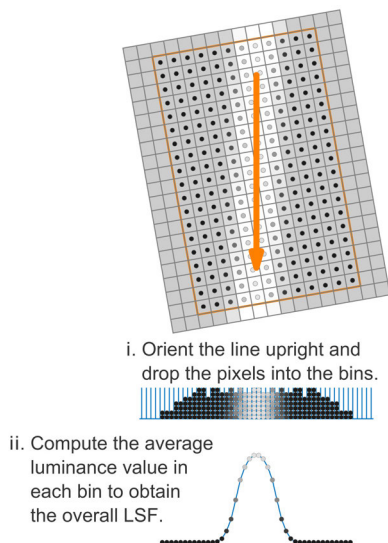


FIGURE 7. Schematic flow diagram of the line-based overall MTF measurement process. A small ROI and wide bins are used here as simple examples.

where x_{LMD} and y_{LMD} are the coordinates of the pixels in the ROI, σ is the standard deviation of the horizontal section of the peak function, and x_0 is the x_{LMD} -intercept of the line. θ and x_0 are optimized to maximize the correlation between the pixel values in the ROI and $v(x_{LMD}, y_{LMD})$ values. In this method, σ is set to $m/3$ to roughly simulate the blurry line profile, where m is the pixel ratio. For the stabilization of this optimization process, σ is not searched, and the fixed value is not used during the rest of the procedure.

D. LUMINANCE PROFILE ESTIMATION

This process involves the estimation of a supersampled luminance profile of the considered line, which is the overall LSF (LSF_{OA}) of the LMD and display. Fig. 7 illustrates the overall LSF estimation procedure. (i) The ROI selected in the previous slant angle procedure is rotated so that the enclosed line is upright. The pixels are then dropped onto the horizontal axis. The axis is divided into $(\text{pixel}_{LMD}/N_{bin})$ -wide bins, where N_{bin} is the oversampling ratio for the LSF_{OA} . The values of the pixels aligned on the axis are grouped into the bins based on the x coordinates of the pixels. (ii) The values of the pixels collected from each bin are averaged to generate a supersampled 1D LSF. This oversampling ($N_{bin} \times$ oversampling) reduces the influence of signal aliasing when estimating the display MTF. The black level is extracted from the LSF. The level may be set to the average of the values on the left and right flat parts of the LSF.

E. OVERALL MTF ESTIMATION

After application of a Tukey (tapered cosine) window to the LSF_{OA} for apodization, a discrete Fourier transform is performed on the function to obtain the OTF. To estimate the overall MTF (MTF_{OA}) of the LMD and display, the modulus of the OTF is normalized to unity at zero frequency.

The underestimation due to the bin-width averaging is compensated for by multiplying the normalized modulus times $|\text{sinc}(\xi_{LMD}/N_{bin})|^{-1}$.

F. COMPENSATION FOR LMD MTF

The MTF of the display (MTF_{DISP}) is estimated from the MTF_{OA} by compensating for the MTF_{LMD} , as follows:

$$MTF_{DISP}(\xi_{LMD}) = MTF_{OA}(\xi_{LMD})/MTF_{LMD}(\xi_{LMD}). \quad (2)$$

where the MTF_{OA} and MTF_{LMD} values were estimated in steps A and E, respectively, at the discrete spatial frequencies of ξ_{LMD} . The division in (2) requires the MTF_{OA} and MTF_{LMD} to have the same frequencies. If this condition is not satisfied, then the MTF_{LMD} should be linearly interpolated.

Finally, ξ_{LMD} is scaled to ξ_{DISP} by a factor of the pixel ratio m estimated in step B to yield MTF_{DISP} as a function of ξ_{DISP} , as follows:

$$MTF_{DISP}(\xi_{DISP}) = MTF_{DISP}(m\xi_{LMD}). \quad (3)$$

IV. SIMULATION

To demonstrate the accuracy and precision of the line-based display MTF measurement method, simulations were performed using a model display with an RGB stripe subpixel arrangement and a model LMD with assumed MTFs. Captured images of a single line on the display screen were computationally generated to simulate the subpixel arrangement of the display and the assumed MTFs of the LMD.

Subsections A and B describe the characteristics of the model display and model LMD, respectively. Subsection C explains the method to produce computer-generated line images of the display screen captured by the LMD. Sub-subsection D presents the simulation results of luminance profile estimates with different pixel ratios. Subsection E demonstrates the accuracy and precision of the display MTF estimation.

A. MODEL DISPLAY

The model display was assumed to have an RGB stripe subpixel array with a black mask. Fig. 8 shows a diagram of a pixel with the arrangement and vertically averaged luminance profile. For simplicity, the luminance values of the RGB subpixels were set to 0.2 (red), 0.7 (green), and 0.1 (blue), which correspond to the rounded values of the luminance ratio of the standard RGB primaries (0.2126:0.7151:0.0722) to the first decimal place. The dimensions of each subpixel were $1/5$ (W) \times $4/5$ (H) of the pixel width. The black mask width was set to $1/10$ of the pixel width to simulate typical UHD displays with a simple fraction, that is, the width ratio of the micro-color filter to the black mask was 2:1. The vertically averaged luminance $LSF_{DISP}(x)$, including the horizontal back mask regions, can be expressed as follows:

$$LSF_{DISP}(x) = 0.8[0.2\text{rect}(5x + 1.5) + 0.7\text{rect}(5x) + 0.1\text{rect}(5x - 1.5)], \quad (4)$$

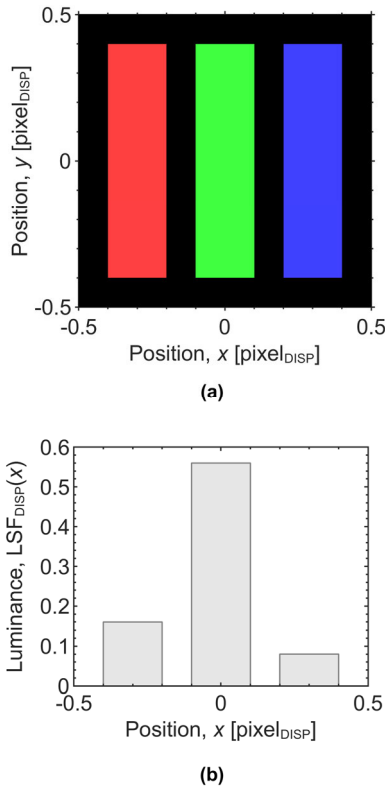


FIGURE 8. RGB stripe arrangement: (a) Layout of the micro-color-filter array and (b) vertically averaged luminance profile.

where the factor of 0.8 is due to the 1/10th of pixel-height at the top and at the bottom, i.e., horizontal black mask regions of each subpixel.

B. MODEL LMD

The MTFs of the LMD were assumed to be $|\text{sinc}(\xi_{x\text{LMD}}, \xi_{y\text{LMD}})|^3$ and $|\text{sinc}(\xi_{x\text{LMD}}, \xi_{y\text{LMD}})|^4$, which are typical of a camera [20], [21]. Here, $\xi_{x\text{LMD}}$ and $\xi_{y\text{LMD}}$ are the horizontal and vertical spatial frequencies of the LMD in cycles/pixel_{LMD}, respectively. These were adopted because a photodetector with a 100% fill factor (i.e., square spatial sensitivity) has an MTF of $|\text{sinc}(\xi_{x\text{LMD}}, \xi_{y\text{LMD}})|$. For computational simplicity, the optical system in front of the photodetector was assumed to have a sinc-based MTF so that the line spread functions were calculated as a rectangular function convolved two and three times with itself, respectively. Fig. 9 shows the MTF curves of the LMD given by $|\text{sinc}(\xi_{x\text{LMD}})|^3$ and $|\text{sinc}(\xi_{x\text{LMD}})|^4$ and the corresponding LSFs of $\text{rect}(x_{\text{LMD}}) * \text{rect}(x_{\text{LMD}}) * \text{rect}(x_{\text{LMD}})$ and $\text{rect}(x_{\text{LMD}}) * \text{rect}(x_{\text{LMD}}) * \text{rect}(x_{\text{LMD}}) * \text{rect}(x_{\text{LMD}})$, respectively. It should be noted that the former LSF is zero for $|x_{\text{LMD}}| > 1.5$ and the latter LSF is zero for $|x_{\text{LMD}}| > 2$.

C. COMPUTER-GENERATED LINE IMAGES

Line images captured by the model LMD for a pixel ratio m and slant angle θ , $L(x_{\text{LMD}}, y_{\text{LMD}}, m, \theta)$, were computationally generated to simulate the MTF_{LMD} of

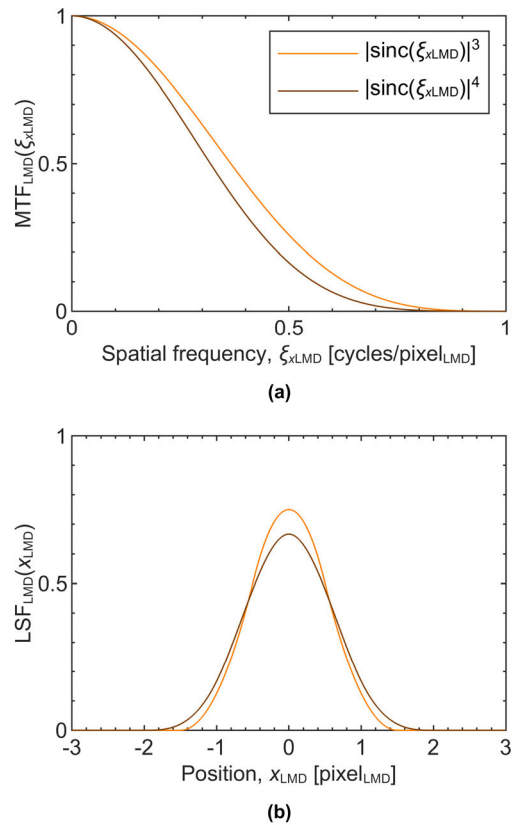


FIGURE 9. Spatial resolution characteristics of the model LMD: (a) MTFs $|\text{sinc}(\xi_{x\text{LMD}})|^3$ and $|\text{sinc}(\xi_{x\text{LMD}})|^4$ and (b) corresponding LSFs.

$|\text{sinc}(\xi_{x\text{LMD}}, \xi_{y\text{LMD}})|^3$ or $|\text{sinc}(\xi_{x\text{LMD}}, \xi_{y\text{LMD}})|^4$ as follows. First, oversampled images $L'(x', y', m, \theta)$ were generated, where (x', y') is the coordinates of the oversampling position. In the present simulation, each LMD pixel was divided into 101×101 squares, and the coordinates of the center of each divided square was set to the oversampling position. Each sample has one of four luminance values of $0.8 \cdot 0.2$ for red, $0.8 \cdot 0.7$ for green, $0.8 \cdot 0.1$ for blue, or 0 for black based on (4). Second, a 101×101 moving average window filter W was applied to $L'(x', y', m, \theta)$. This filter was repeated as many times as the order of the sinc function of the assumed MTF (i.e., three or four times). Finally, $L_{\text{LMD}}'(x', y', m, \theta)$ was downsampled by taking one sample at the center of the 101×101 sampling grid of each square to yield $L_{\text{LMD}}(x_{\text{LMD}}, y_{\text{LMD}}, m, \theta)$.

Fig. 10 shows 200×200 -pixel images of a line with a slant angle θ of 3° computationally generated using the MTF_{LMD} of $|\text{sinc}(\xi_{x\text{LMD}}, \xi_{y\text{LMD}})|^3$ for pixel ratios m of 1, 3, 10, and 30. The images for the MTF_{LMD} of $|\text{sinc}(\xi_{x\text{LMD}}, \xi_{y\text{LMD}})|^4$ are not included in this paper owing to the difficulty of distinguishing between the images of the two MTFs when they are compressed or printed.

D. LUMINANCE PROFILE

The overall luminance profiles $\text{LSF}_{\text{OA}}(x)$ were obtained by the proposed line-based method for the MTF_{LMD} of

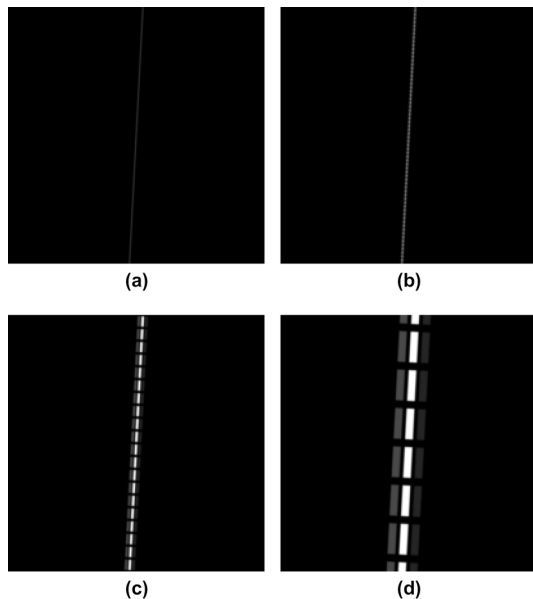


FIGURE 10. Computer-generated 200×200 -pixel images of a vertical line displayed on the screen with the RGB-stripe array with the MTF of $|\text{sinc}(\xi_{x\text{LMD}}, \xi_{y\text{LMD}})|^3$ for pixel ratios of (a) 1, (b) 3, (c) 10, and (d) 30.

$|\text{sinc}(\xi_{x\text{LMD}}, \xi_{y\text{LMD}})|^3$ and $|\text{sinc}(\xi_{x\text{LMD}}, \xi_{y\text{LMD}})|^4$ and m values of 1, 3, 10, and 30. Fig. 11 compares the discrete LSF_{OA} values with their reference profiles. The oversampling ratio N_{bin} for the oversampling of LSF_{OA} was set to 8; hence, there are 8 markers per $\text{pixel}_{\text{LMD}}$. The continuous reference profiles were computed using the convolution of the vertically averaged horizontal luminance profile of the RGB subpixels defined in (4) and LSF_{LMD} , as follows:

$$\text{LSF}_{\text{OA}}(x) = \text{LSF}_{\text{DISP}}(x/m) * \text{LSF}_{\text{LMD}}(x), \quad (5)$$

where x is the position in $\text{pixel}_{\text{LMD}}$. The overall luminance profiles obtained by this 1D convolution are identical to those obtained by 2D convolution. It should be noted that in the actual simulation, $\text{LSF}_{\text{LMD}}(x)$ in (5) was approximated by $\text{LSF}_{\text{LMD}}(x_{\text{LMD}})$, as shown in Fig. 9b. For pixel ratios of 1 and 3, the discrete LSF_{OA} values computed by the simulation of the line-based method qualitatively agree well with the reference values. It can be also observed that the vertical black mask regions between the RGB subpixels are completely blurred. For pixel ratios of 10 and 30, on the other hand, the vertical black mask regions between the subpixels cause dents in the luminance profile. Furthermore, the simulated values fluctuate because of the horizontal black mask regions. This unevenness of the LSF_{OA} caused by the black mask at high pixel ratios, however, does not affect the display MTF estimation because the spatial frequency components of the black mask are beyond the Nyquist frequency.

E. ACCURACY AND PRECISION OF DISPLAY MTF ESTIMATION

The discrete $\text{MTF}_{\text{DISP}}(\xi_{\text{DISP}})$ were estimated by the proposed line-based method. Fig. 12 compares the values with the

reference MTF curve. The reference MTF was computed as the modulus of the Fourier transform of the $\text{LSF}_{\text{DISP}}(x)$ normalized to unity at zero frequency, as follows:

$$\text{MTF}_{\text{DISP}}(\xi_{\text{DISP}}) = |\text{sinc}(0.2\xi_{\text{DISP}})(0.2e^{j0.6\pi\xi_{\text{DISP}}} + 0.7 + 0.1e^{-j0.6\pi\xi_{\text{DISP}}})|. \quad (6)$$

The estimated discrete MTF_{DISP} for a pixel ratio of 30 can be observed to be poorly sampled because the spatial frequency scaling from ξ_{LMD} to ξ_{DISP} based on (3) is too large. The sampling interval $\Delta\xi_{\text{DISP}}$ of the spatial frequency ξ_{DISP} in cycles/ $\text{pixel}_{\text{DISP}}$ is proportional to the pixel ratio m , as follows:

$$\Delta\xi_{\text{DISP}} = m/w, \quad (7)$$

where w is the length of the obtained LSF_{OA} in $\text{pixel}_{\text{LMD}}$. For a square ROI, measuring $h \times h$ pixels, w is approximated by the horizontal width of the ROI rotated by θ as $w \approx h(|\cos \theta| + |\sin \theta|)$. In the present simulation ($h = 200$, $\theta = 3^\circ$), w is approximated as 210 $\text{pixel}_{\text{LMD}}$, and $\Delta\xi_{\text{DISP}}$ is 0.143 cycles/ $\text{pixel}_{\text{DISP}}$ for $m = 30$. The poor sampling can be proportionally improved by using a wider ROI.

For a pixel ratio of 1, on the other hand, the error of the MTF estimates deviate from the reference toward the Nyquist frequency. This originates from the thinness of the line, which results in the provision of less information. In this case, using a longer line in a given ROI would reduce the error.

For critical investigation of the accuracy of the proposed line-based method, the display MTF at the Nyquist frequency was estimated for different conditions. The MTF_{DISP} was linearly interpolated from the discrete MTF_{OA} with the compensation of the MTF_{LMD} of $|\text{sinc}(\xi_{x\text{LMD}}, \xi_{y\text{LMD}})|^3$ and $|\text{sinc}(\xi_{x\text{LMD}}, \xi_{y\text{LMD}})|^4$ at 0.5 cycles/ $\text{pixel}_{\text{DISP}}$. The correct slant angle and pixel ratio values were manually set in the present simulation to eliminate the errors that could otherwise originate from their values.

Fig. 13 shows the MTF_{DISP} at the Nyquist frequency ($\xi_{\text{DISP}} = 0.5$) as estimated by the proposed line-based method for pixel ratios of 1 to 30 at intervals of 0.1. Each image was generated with 200×200 pixels and a slant angle of 3° . The modulation level starts to fluctuate below the reference value when the pixel ratio exceeds 10. This is attributable to the linear interpolation between the poorly sampled points (i.e., large $\Delta\xi_{\text{DISP}}$) of the concave-down MTF curve.

Fig. 14 shows the MTF_{DISP} at the Nyquist frequency for $200 \times h$ -pixel generated images with a pixel ratio of 1, where h ranges from 200 to 1000. The modulation value fluctuates but approaches the reference value as h increases.

Fig. 15 shows the estimated MTF_{DISP} at the Nyquist frequency for slant angles of 1° – 4° at intervals of 0.01° . Each utilized image had 200×200 pixels with MTF_{LMD} of $|\text{sinc}(\xi_x, \xi_y)|^3$ and $|\text{sinc}(\xi_x, \xi_y)|^4$ and a pixel ratio of 3. As can be observed from the figure, high precision was achieved mostly within $\pm 0.1\%$.

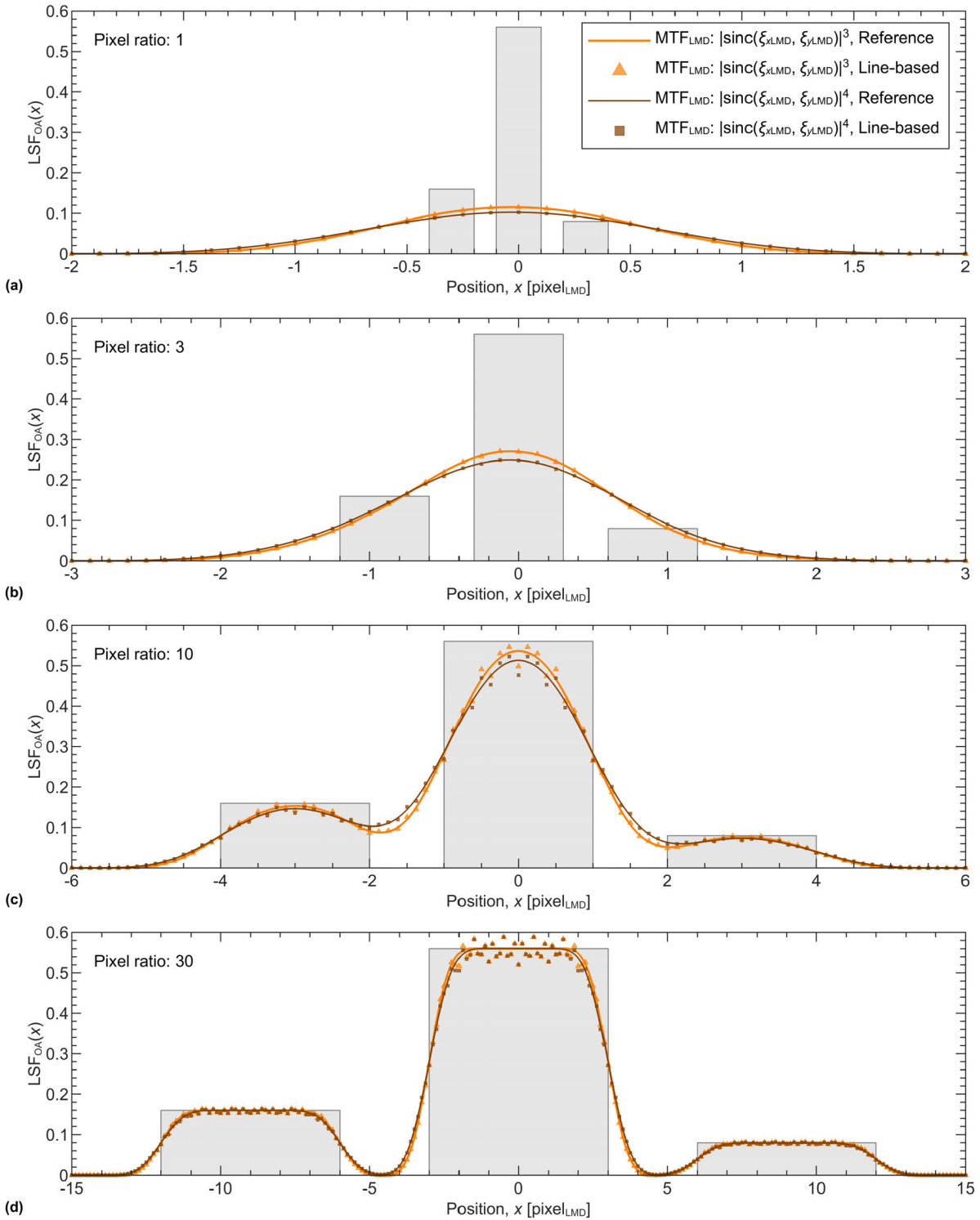
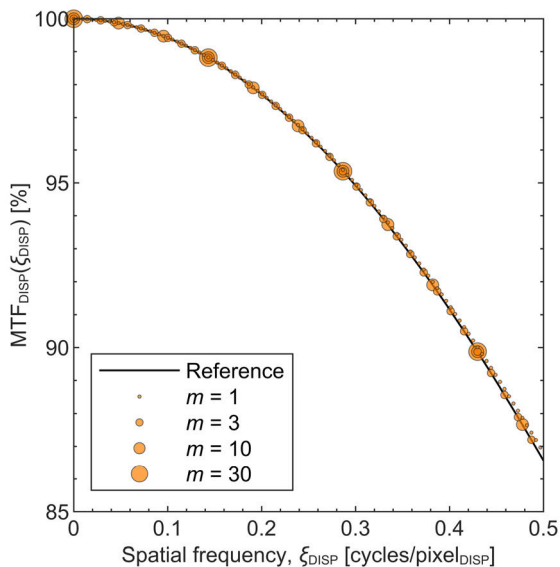


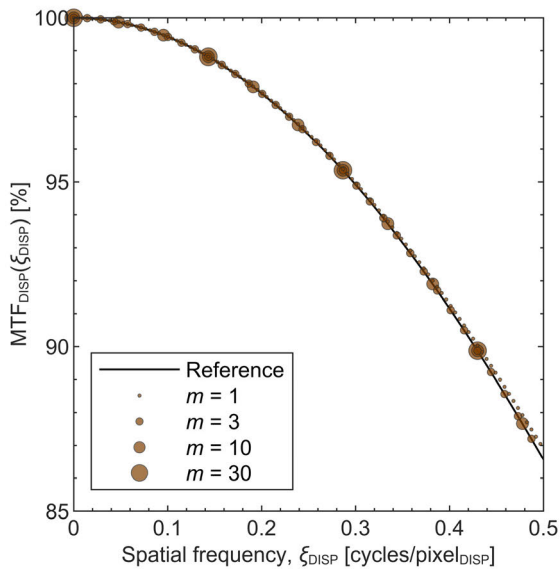
FIGURE 11. Comparison of the overall luminance profiles obtained by the proposed line-based method (markers) with their reference values (orange and brown solid lines) using the MTF_{LMD} of $|\text{sinc}(\xi_{xLMD}, \xi_{yLMD})|^3$ and $|\text{sinc}(\xi_{xLMD}, \xi_{yLMD})|^4$ for pixel ratios of (a) 1, (b) 3, (c) 10, and (d) 30. The light gray areas indicate the vertically averaged horizontal luminance profiles of the RGB subpixels (Fig. 8b).

The analyses of the accuracy and precision of the proposed line-based method in the present work were limited. In reality, the accuracy and precision depend on the specific combination of all the relevant factors, namely, the MTF of the

LMD, subpixel arrangement of the display, pixel ratio, ROI size, slant angle, binning size, and binning phase. An analysis that considers all these factors would be very complex and is beyond the scope of the present study. However, the precision



(a)



(b)

FIGURE 12. $MTF_{DISP}(\xi_{DISP})$ obtained by the proposed line-based method using the MTF_{LMD} of (a) $|\text{sinc}(\xi_{xLMD}, \xi_{yLMD})|^3$ and (b) $|\text{sinc}(\xi_{xLMD}, \xi_{yLMD})|^4$ for pixel ratios of 1, 3, 10, and 30, compared with the reference values.

of the proposed method may be significantly improved by averaging the MTFs obtained for multiple offsets of the bins in the binning procedure [15].

F. MTF FOR COLOR LINES

The proposed line-based method can also be applied to colored lines. Fig. 16 compares the MTF_{DISP} for green, cyan, magenta, and yellow vertical lines and a white horizontal line rendered by the model display. The colors were simulated by setting the corresponding RGB luminance values of 0.2, 0.7, and/or 0.1 to zeros in (6). Each image contained

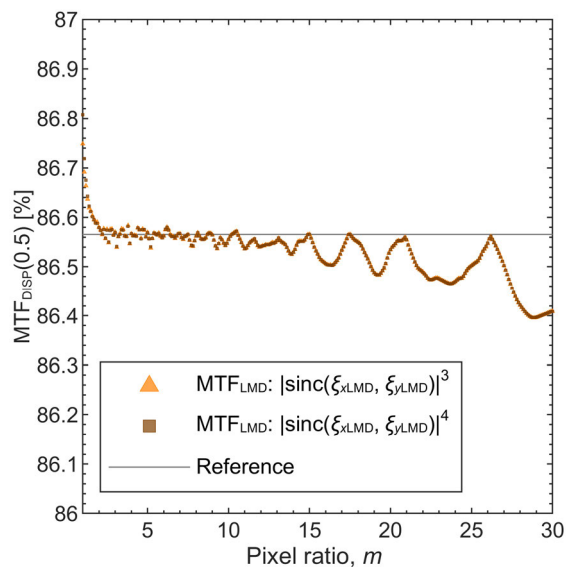


FIGURE 13. MTF_{DISP} at the Nyquist frequency estimated by the proposed line-based method using 200×200 -pixel images generated with pixel ratios of 1 to 30 at intervals of 0.1.

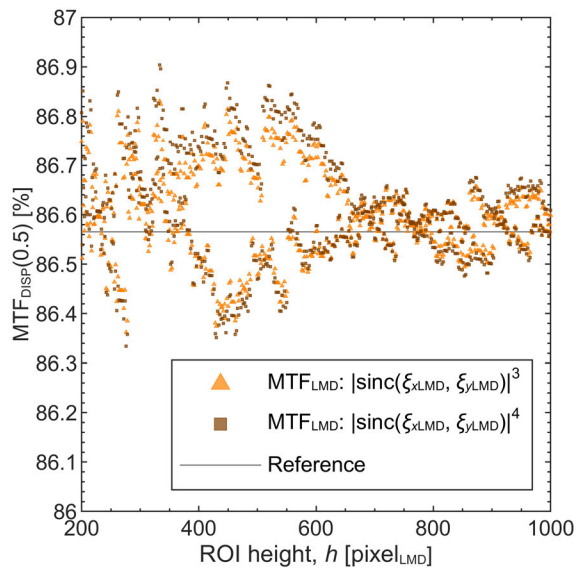


FIGURE 14. MTF_{DISP} at the Nyquist frequency estimated by the proposed line-based method using $200 \times h$ -pixel images generated with a pixel ratio of 1.

200×200 pixels with MTF_{LMD} of $|\text{sinc}(\xi_x, \xi_y)|^3$ or $|\text{sinc}(\xi_x, \xi_y)|^4$ and a pixel ratio of 3. The MTFs for the blue and red vertical lines are not shown because they are identical to that for the green vertical line. The reference MTF for the horizontal line was calculated as $|\text{sinc}(0.8\xi_{DISP})|$, which is independent of the color in the case of an RGB stripe layout (Fig. 8). As can be seen, the discrete MTF_{DISP} values are on the curve of reference MTF regardless of the MTF_{LMD} .

V. DISCUSSION

A. PRACTICAL MEASUREMENT CONDITIONS

As is mentioned in the Introduction, for the ICDM contrast modulation method, a pixel ratio of 30 is recommended.

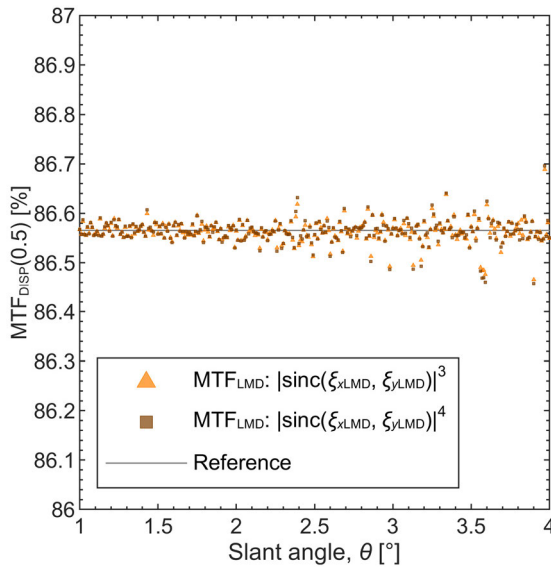


FIGURE 15. MTF_{DISP} at the Nyquist frequency obtained by the proposed line-based method using 200×200 -pixel images and slant angles of 1° to 4° at intervals of 0.01° .

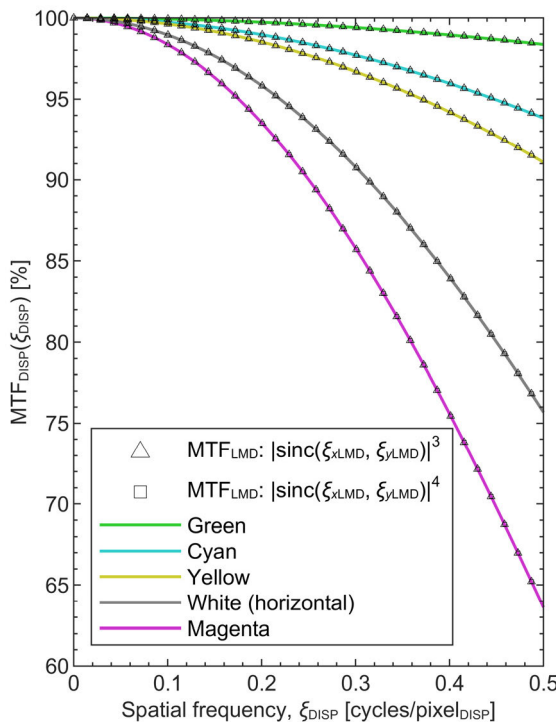


FIGURE 16. $MTF_{DISP}(\xi_{DISP})$ estimated for green, cyan, magenta, and yellow vertical lines and a white horizontal line using the proposed line-based method compared with their reference values (solid lines).

Some devices may require a higher pixel ratio [5]. However, a high pixel ratio usually requires a short working distance, which causes reflection from the objective lens to the display and the possibility of considerable errors due to stray light within the optics of the LMD [2]. On the other hand, it has been found that the simulation results of the proposed

line-based display MTF measurement method are accurate and precise for a wide range of pixel ratios. In particular, the lower range of the pixel ratios enables the use of a smaller lens with a longer working distance.

B. CONTRAST MODULATION VERSUS MTF

Here, a monochromatic display pixelated in a square grid pattern is assumed. The black level is zero. Interpixel crosstalk does not exist. If the display has a “point pixel,” i.e., a fill factor of 0%, the contrast modulation is 100%. In this case, the MTF of the point pixel is unity. Otherwise, if the display has a square pixel without black mask, i.e., a fill factor of 100%, the luminance profiles is represented as a one-pixel_{DISP}-wide rectangular function. The grille pattern yields a perfect square wave profile, resulting in a contrast modulation of 100% again. On the other hand, the line-based display MTF has a function of $|\text{sinc}(\xi_{DISP})|$ with a modulation of 63.7% at the Nyquist frequency. That means the contrast modulation method cannot differentiate the sharpness that depends on the fill factor or interpixel luminance profile.

C. REFERENCE MTF

A few sinc-based functions are considered for the display MTF of the reference. As mentioned in the previous subsection, a pixel with a fill factor of 100% has an MTF of $|\text{sinc}(\xi_{DISP})|$. If a display pixel has a two-pixel_{DISP}-wide triangular luminance profile, the grille pattern yields a triangular-wave luminance profile, having a contrast modulation of 50%, which is identical to CTA’s criterion [4]. The corresponding MTF for the triangular function is $|\text{sinc}(\xi_{DISP})|^2$ with a modulation of 40.5% at the Nyquist frequency. Thus, sinc-based functions can be employed as standard guides for evaluating display MTFs.

D. MEASUREMENT SYSTEM IMPLEMENTATION

In the present work, a square ROI measuring 200×200 pixels was mainly used in the simulation of the proposed line-based method. This ROI size has been well tested for accuracy and precision in the measurement of the MTFs of LMDs [15]. The small ROI size significantly reduces the computational cost and enables the use of an affordable low-resolution camera. In essence, a camera with a low pixel count sensor, such as a VGA camera, can have large size pixels that capture more light per pixel. In addition, unlike the ICDM edge-based method, the proposed line-based display MTF measurement method does not require smoothing of the ESF and subsequent conversion into the LSF. All these features of the proposed method are advantageous for real-time measurement.

Real-time MTF measurement improves the measurement accuracy and efficiency. According to the ISO 12233 standard, the camera should be accurately focused through a series of image captures using different focus settings that provide the highest average modulation level. Usually, camera MTF measurement is a multistep process that includes a cycle of shooting with various focuses to find the best one for each condition such as iris and focal length, then transferring



FIGURE 17. Prototype display MTF measurement system.

the data to a computer, and analyzing it. This repetitive and error-prone procedure can be streamlined by the real-time camera MTF measurement [21]. The proposed line-based display MTF measurement method can also be implemented by computer software for real-time measurement, with the slant angle assumed to be constant during the measurement because the algorithm is similar to that of the edge-based camera MTF measurement method.

E. DEMONSTRATION

A prototype measurement system was developed to demonstrate the accuracy and computational efficiency of the proposed line-based display MTF measurement method. The system was exhibited in the Innovation Zone (I-Zone) at the Society for Information Display (SID) Display Week in 2020. Fig. 17 shows the prototype. A GenICam compliant area scan camera (acA720-520um, Basler AG, Germany) with a 720×540 -pixel monochrome CMOS image sensor (IMX287, Sony Semiconductor Solutions Corp., Japan) having a $\text{pixel}_{\text{LMD}}$ of $6.9 \mu\text{m}$ was used with a C-mount 50-mm fixed focal lens (LM50JC10M, Kowa Company Ltd., Japan) at $f/5.6$. The camera was connected via USB to a tablet PC (HP Elite x2 1013 G3, HP Inc., CA) with Windows 10 x64/1.7 GHz quad-core Intel Core i5 processor/16 GB RAM. The camera was mounted on a rack and pinion stage. To measure the MTFs of the camera and the display, the real-time MTF measurement software [21] was modified to support the GenICam standard and the proposed display MTF measurement method.

A 23.8-inch 4K liquid crystal display (LCD) with an RGB stripe subpixel arrangement having a $\text{pixel}_{\text{DISP}}$ of 0.13725 mm was used as the display under test. A vertical white line was displayed on the screen and captured by the camera continuously, that is, each time a display MTF measurement was performed, one image was acquired by the PC. The display MTF measurement was performed at about 10 frames/sec, which was fast enough to accurately adjust the focus distance of the camera based on the MTF results. After focus adjustment, several images were averaged to reduce the sensor noise. The display MTF measurement was conducted for pixel ratios of 2.0, 4.0, and 8.9, the last

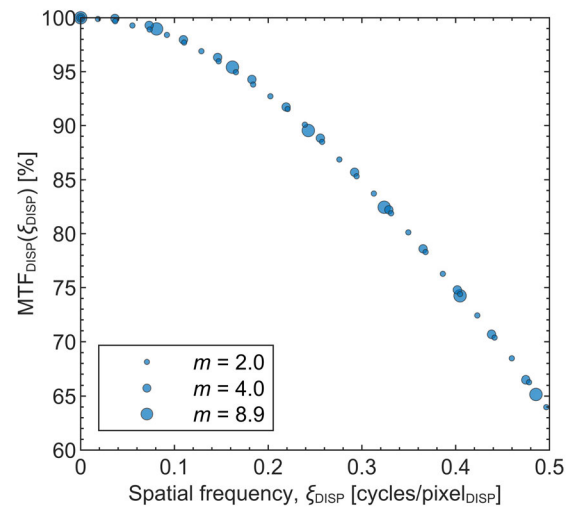


FIGURE 18. $\text{MTF}_{\text{DISP}}(\xi_{\text{DISP}})$ of the LCD measured by the prototype system for pixel ratios of 2.0, 4.0, and 8.9.

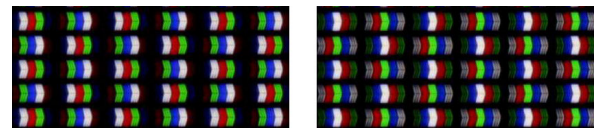


FIGURE 19. Alternating vertical lines of black and white pixels with two different phases [2].

of which was limited by the minimum working distance of the lens of 10 mm. A common central 100×200 -pixel ROI was used for each pixel ratio. Fig. 18 shows the MTF results, where they approximately trace an identical curve.

F. CONSTRAINTS OF LINE-BASED METHOD

In the present simulation, the interpixel crosstalk (mentioned in Section I) as well as crosstalk between subpixels caused by the front surface diffusers were not considered. The crosstalk attenuates the modulations and causes smaller aliasing artifacts. Therefore, the effect on the resultant MTF is less critical in terms of accuracy and precision.

Many modern displays utilize subpixel arrangements wherein the subpixel density depends on the subpixel type or color. If the display system is assumed to be shift-invariant to the discrete input image data, the MTF will be estimated accurately. However, some displays have a line-by-line alternating subpixel arrangement with different line responses depending on the phase [2], as shown in Fig. 19. In this case, the line response depends on the phase of the input line, and it becomes necessary to measure the line in different phases to ensure the accuracy of the proposed method.

It is noteworthy that, when the signal is under- or oversampled in a digital imaging device to accommodate the signal data within the physical pixels of the device, the number of cycles per pixel unit based on the signal is employed. However, the discrete shift-invariance assumption for pixelated displays fails when the display has different line responses [22].

VI. CONCLUSION

The increasing application of UHD imaging and the proliferation of the associated devices has resulted in the need for more efficient and realistic imaging. This paper proposed a new line-based display MTF measurement method. The proposed method was demonstrated for vertical and horizontal white and non-white lines with typical RGB stripe subpixel arrangement by computer simulation and was confirmed to yield accurate and precise results for a wide range of pixel ratios. It particularly enables the use of a significantly lower pixel ratio with a smaller lens and longer working distance. Further, the use of a small ROI significantly reduces the computational cost and enables display MTF measurement using an affordable low-resolution camera. These features of the proposed method facilitate real-time MTF measurement, as demonstrated using the prototype system, promising accurate and efficient evaluation of the spatial imaging performance of the entire sampled imaging system and its constituent subsystems, in a manner consistent with the MTF metric.

ACKNOWLEDGMENT

The author would like to thank Dr. K. Kälantär (SID Fellow) of Global Optical Solutions (Japan) for valuable discussions.

REFERENCES

- [1] K. Masaoka, Y. Nishida, M. Sugawara, E. Nakasu, and Y. Nojiri, "Sensation of realism from high-resolution images of real objects," *IEEE Trans. Broadcast.*, vol. 59, no. 1, pp. 72–83, Mar. 2013.
- [2] M. E. Becker, "Measurement of visual resolution of display screens," in *SID Symp. Dig. Tech. Pap.*, May 2017, vol. 48, no. 1, pp. 915–918.
- [3] *Information Display Measurements Standard, Version 1.03*, Soc. Inf. Display, Campbell, CA, USA, 2012.
- [4] Consumer Technology Association. (2019). *8K UHD Display Characteristics*. [Online]. Available: <http://cdn.cta.tech/cta/media/media/membership/pdfs/cta-8k-uhd-display-characteristics-july-2019.pdf>
- [5] K. Masaoka, "Accuracy and precision limitations in measuring luminance modulation for pixelated displays," *Opt. Express*, vol. 28, no. 19, pp. 27865–27872, Sep. 2020.
- [6] *Information Display Measurements Standard, Version 1.03c*, Soc. Inf. Display, Campbell, CA, USA, 2016.
- [7] S. Triantaphillidou and R. E. Jacobson, "Measurements of the modulation transfer function of image displays," *J. Imag. Sci. Technol.*, vol. 48, no. 1, pp. 58–65, Jan./Feb. 2004.
- [8] A. S. Chawla, H. Roehrig, J. Fan, and K. Gandhi, "Real-time MTF evaluation of displays in the clinical arena," *Proc. SPIE*, vol. 5029, pp. 734–745, May 2003.
- [9] T. H. Kim, Y. W. Lee, H. M. Cho, and I. W. Lee, "Evaluation of image quality of color liquid crystal displays by measuring modulation transfer function," *Opt. Eng.*, vol. 38, no. 10, pp. 1671–1678, Oct. 1999.
- [10] B. Kaur, J. Olson, and E. A. Flug, "Display MTF measurements based on scanning and imaging technologies and its importance in the application space," *Proc. SPIE*, vol. 9820, May 2016, Art. no. 98200Y.
- [11] K. Ichikawa, Y. Kodera, and H. Fujita, "MTF measurement method for medical displays by using a bar-pattern image," *J. Soc. Inf. Display*, vol. 14, no. 10, pp. 831–837, Oct. 2006.
- [12] A. Vetsuypens, C. Marchessoux, and T. Kimpe, "A novel methodology for display 2D MTF evaluation: The pixel spread function (PxSF)," *Proc. SPIE*, vol. 7627, Feb. 2010, Art. no. 762714.
- [13] G. D. Boreman, "MTF in electro-optical systems," in *Modulation Transfer Function in Optical and Electro-optical Systems*. Bellingham, WA, USA: SPIE, vol. 2001, pp. 31–58.
- [14] *Photography-Electronic Still Picture Imaging-Resolution and Spatial Frequency Responses*, Standard ISO 12233, 2017.
- [15] K. Masaoka, "Accuracy and precision of edge-based modulation transfer function measurement for sampled imaging systems," *IEEE Access*, vol. 6, pp. 41079–41086, Jul. 2018.
- [16] C. Infante, "On the modulation transfer function of matrix displays," *J. Soc. Inf. Display*, vol. 1, no. 4, pp. 449–450, Dec. 1993.
- [17] *Parameter Values for Ultra-High Definition Television Systems for Production and International Programme Exchange*, Standard Recommendation ITU-R BT.2020-2, 2015.
- [18] K. Masaoka, T. Yamashita, Y. Nishida, and M. Sugawara, "Modified slanted-edge method and multidirectional modulation transfer function estimation," *Opt. Express*, vol. 22, no. 5, pp. 6040–6046, 2014.
- [19] J. B. Phillips and H. Eliasson, *Camera Image Quality Benchmarking*. Hoboken, NJ, USA: Wiley, 2018, pp. 200–201.
- [20] N. Koren. (2011). *Understanding Image Sharpness, Part 2: Resolution and MTF Curves in Scanners and Sharpening*. [Online]. Available: <http://www.normankoren.com/Tutorials/MTF2.html>
- [21] K. Masaoka, K. Arai, and Y. Takiguchi, "Realtime measurement of ultrahigh-definition camera modulation transfer function," *SMPTE Motion Imag. J.*, vol. 127, no. 10, pp. 14–22, Nov. 2018.
- [22] D. M. Hoffman, C. McKenzie, B. Koprowski, A. Iqbal, and N. Balram, "Aligning content rendering resolution and feature size with display capability in near-eye display systems," *J. Soc. Inf. Display*, vol. 27, no. 4, pp. 207–222, Apr. 2019.



KENICHIRO MASAOKA received the B.S. degree in electronics engineering, the M.S. degree in energy engineering, and the Ph.D. degree in engineering from the Tokyo Institute of Technology, Japan, in 1994, 1996, and 2009, respectively. He is currently a Principal Research Engineer with the NHK Science and Technology Research Laboratories, Tokyo, Japan. He worked with Professors Mark Fairchild and Roy Berns during a six-month residency as a Visiting Scientist at the Munsell Color Science Laboratory, Rochester Institute of Technology, in 2012. His research interests include color science and digital imaging systems. In 2017, he received a Special Recognition Award from the Society for Information Display (SID) for his leading contributions to the research and development of a wide-color-gamut UHD-TV display system and gamut-area metrology. In 2019, he received the Journal Certificate of Merit from the Society of Motion Picture and Television Engineers (SMPTE) for his paper titled "Realtime Measurement of Ultrahigh-Definition Camera Modulation Transfer Function." Since 2018, he has been the Chair of the Subcommittee on Color Metrology of the International Committee for Display Metrology (ICDM), a part of the SID Definitions and Standards Committee charged with setting standards for display metrology.

• • •